Title

Oxylipin concentration shift in exhaled breath condensate (EBC) of SARS-CoV-2 infected patients

Journal

Journal of Breath Research, 17(4)

ISSN

1752-7155

Authors

Borras, Eva

McCartney, Mitchell M

Rojas, Dante E

et al.

Publication Date

2023-10-01

DOI

10.1088/1752-7163/acea3d

Peer reviewed

HHS Public Access

Author manuscript

J Breath Res. Author manuscript; available in PMC 2024 August 07.

Published in final edited form as:

J Breath Res. ; 17(4): . doi:10.1088/1752-7163/acea3d.

Oxylipin concentration shift in exhaled breath condensate of SARS-CoV-2 infected patients

Eva Borras[1,2,6], **Mitchell M. McCartney**[1,2,3,6], **Dante E. Rojas**[1,2], **Tristan L Hicks**[1,2], **Nam K Tran**[4,2], **Tina Tham**[5,2], **Maya M Juarez**[2,5], **Lisa Franzi**[2,5], **Richart W. Harper**[2,3,5], **Cristina E. Davis**[1,2,3], **Nicholas J. Kenyon**[2,3,4,*]

[1]Mechanical and Aerospace Engineering, One Shields Avenue, University of California, Davis, Davis, California, USA

[2]UC Davis Lung Center, University of California Davis, CA

[3]VA Northern California Health Care System, 10535 Hospital Way, Mather, CA 95655, USA.

[4]Department of Pathology and Laboratory Medicine, UC Davis, Sacramento CA, USA

[5]Department of Internal Medicine, 4150 V Street, Suite 3400, University of California, Davis, Sacramento, CA 95817, USA

[6]These authors contributed equally: Eva Borras, Mitchell M. McCartney

Abstract

Infection of airway epithelial cells with severe acute respiratory coronavirus 2 (SARS-CoV-2) can lead to severe respiratory tract damage and lung injury with hypoxia. It is challenging to sample the lower airways noninvasively and the capability to identify a highly representative specimen that can be collected in a non-invasive way would provide opportunities to investigate metabolomic consequences of COVID-19 disease. In the present study, we performed a targeted metabolomic approach using liquid chromatography coupled with high resolution chromatography (LC-MS) on exhaled breath condensate (EBC) collected from hospitalized COVID-19 patients (COVID+) and negative controls, both non-hospitalized and hospitalized for other reasons (COVID-). We were able to noninvasively identify and quantify inflammatory oxylipin shifts and dysregulation that may ultimately be used to monitor COVID-19 disease progression or severity and response to therapy. We also expected EBC-based biochemical oxylipin changes associated with COVID-19 host response to infection.

The results indicated ten targeted oxylipins showing significative differences between SAR-CoV-2 infected EBC samples and negative control subjects. These compounds were prostaglandins A2 and D2, LXA4, 5-HETE, 12-HETE, 15-HETE, 5-HEPE, 9-HODE, 13-oxoODE and 19(20)-EpDPA, which are associated with specific pathways (i.e. P450, COX, 15-LOX) related to

*Corresponding author: Prof. Nickolas J. Kenyon (njkenyon@ucdavis.edu).

Ethical Statement

This study was approved and conducted under institutional IRB approved human subjects protocols at the University of California, Davis (1636182-2) and VA Mather Hospital, Northern California Health Care System (152048).

The research was conducted in accordance with the principles embodied in the Declaration of Helsinki and in accordance with local statutory requirements.

All participants gave written informed consent to participate in the study

inflammatory and oxidative stress processes. Moreover, all these compounds were up-regulated by COVID+, meaning their concentrations were higher in subjects with SAR-CoV-2 infection. Given that many COVID-19 symptoms are inflammatory in nature, this is interesting insight into the pathophysiology of the disease. Breath monitoring of these and other EBC metabolites presents an interesting opportunity to monitor key indicators of disease progression and severity.

Keywords

Exhaled breath condensate (EBC); COVID 19; SARS-CoV-2; metabolomics; breath analysis; LC-qTOF

1. Introduction

The ongoing pandemic of COVID-19 is a global threat with over 600 million confirmed cases and over 6 million deaths around the world so far by November 2022 [1]. SARS-CoV-2 is a coronavirus that causes a respiratory disease called COVID-19. This viral infection can lead to a variety of complex heterogenous pathologies and long-term outcomes. Respiratory diseases with upper and lower respiratory problems and acute lung damage are the most common effects, but it can also affect multiple other organs [2].

Current tests to diagnose COVID-19 are based on direct detection of the SARS-CoV-2 virus, mainly using nasopharyngeal swab samples and reverse transcription polymerase chain reaction (RT-PCR) amplification of the virus offline [3]. There have also been a proliferation of rapid over-the-counter antibody-based lateral flow assays as well. Both tests can have false negative rates that vary by assay, and sometimes additional specimens of the lower respiratory tract are recommended in subjects with comorbidities associated with poorer clinical outcomes [4]. Although specimens from the lower respiratory tract, such as sputum, tracheal aspirates or bronchoalveolar lavage fluid, have better sensitivity to SARS-CoV-2 detection [5], they require a significantly more invasive collection process. The exhaled breath condensate (EBC) fraction of exhaled breath has been shown to include virus particles that can be detected using molecular assay techniques [6]. We also know from prior work that metabolites in EBC can reflect blood-based concentrations compounds [7], although at lower concentrations. Prior work has also demonstrated EBC metabolite shifts that correlate with clinical outcomes in animal environmental health exposures [8] and with specific disease progression [9]. We are now positioned to use EBC as an adjacent measurement to commonly used diagnostics, and blood-based assays for specific health queries.

EBC is a liquid or frozen matrix that contains evaporated and condensed particles and aerosols reflecting the metabolites found in the airway surface liquid and lung environment [10]. EBC is obtained by cooling the exhaled air on a cold surface of the condenser (e.g. RTube, TurboDECCS, and EcoScreen) [11]. Besides being a non-invasive technique, EBC collection is also inexpensive, easy to perform, with a variable amount of times required for the collection depending on the sampler used. EBC is mainly formed by water vapor (>99%) which can contain volatile organic compounds (VOCs). However, the EBC droplets also contain a variety of larger non-volatile metabolites (e.g. fatty acids, cytokines, leukotrienes,

prostaglandins), proteins, salts, and microorganisms, such as viral or bacterial particles [12, 13].

Several studies have now demonstrated the presence of the SARS-CoV-2 virus in EBC [14–17]. Most of these studies are focused on the detection of the viral loads in EBC collected from patients with SARS-CoV-2, but detection rates are widely varied remaining inconsistent and limited [18–20]. However, since EBC also reflects the metabolic host response to viral infection, EBC has the potential to mirror those blood metabolic states and its analysis can be used to diagnose, monitor, or detect biomarkers for respiratory illnesses [13, 21–25]. Still not completely understood, COVID-19 is associated with several physiological changes caused by different conditions. These conditions can be related to the metabolic processes causing changes on optimal concentrations or changing the shifts of molecular species in the body. Some previous studies have demonstrated these changes can cause alterations of the metabolome, lipidome and proteome, and those can be detected in blood [21, 24] and breath [26, 27] from patients with SARS-CoV-2. To our knowledge, this is the first reported study of EBC-based biochemical oxylipin changes associated with COVID-19 host response to infection. This is a critical first step to identify airway inflammation and oxidative stress related biomarkers to understand the effects of the disease. Although the COVID-19 pandemic has created an urgent need for rapid, accurate, highly sensitive and specific diagnostic tests for novel respiratory pathogens, it is also important to develop personalized medicine for this type of patients [22], and EBC is positioned to fill that role.

LC-MS is one of the most sensitive and reliable methods to perform metabolomic analysis, especially of EBC samples [28–30]. When used for targeted approaches with a hypothesis-driven goal, the analysis is based the quantification of *a priori* defined compounds of interest. In this study, we focus on compounds related to inflammatory and oxidative stress processes [25]. The aim of this study is to assess if EBC inflammatory and non-inflammatory metabolites are altered in hospitalized patients with confirmed COVID-19 infection as defined by RT-PCR (COVID+) compared to negative controls (COVID-). Specifically, we hypothesized that a profile of inflammatory oxylipins are measurable in EBC, and are different in COVID+ patients and COVID− controls. EBC samples were collected using condensate collection devices previously reported [11, 31]; and the EBC samples were lyophilized, reconstituted, and then analyzed using LC-MS. Additionally, to reduce the threat of infectious exposure, all potential virus load from EBC samples was inactivated using a previously described methodology appropriate for mass spectrometry sample analysis [6].

2. Material and methods

2.1. Clinical study

All subjects that participated in this cross-sectional, case-control study signed a written informed consent obtained following a previously approved protocol for human subjects research (VA IRB #1582048, UC Davis IRB #1636182). A total of 35 volunteers were recruited from either the Veteran's Affairs Northern California Health Care System Hospital in Mather, CA or the UC Davis Medical Center (Sacramento, CA), and from the UC Davis

main campus between February 2021 to January 2022. All participants were age 18 and older and demographic data (age, race, ethnicity, COVID-19 vaccination status, medical history, symptoms, and more) was obtained with a detailed questionnaire or a review of the medical records.

All COVID(+) participants cohort were hospitalized, diagnosed within the past two weeks with COVID-19 with SARS-CoV-2 mRNA detected via reverse transcription PCR (RT-PCR), and receiving a variety of COVID-19 treatments. All subjects were in the relatively acute phase of their illness. No subject was considered to be re-hospitalized with sub-chronic or long-term COVID syndromes.

Among the control subjects, not all participants were tested for SARS-CoV-2 at the time of breath collection. Eight of the 21 control subjects were hospitalized for other conditions and diagnosed with a negative PCR test for SARS-CoV-2. The rest of the control participants were non-hospitalized volunteers with no upper respiratory symptoms. Hospitalized subjects in the control group were admitted with a variety of diagnoses. While they had symptoms of dyspnea at times, this was often secondary to non-pulmonary diagnoses. The most common diagnosis at the time of admission was sepsis (N=3), either secondary to abdominal source (appendicitis, cholecystitis) or undefined. Other diagnoses included diabetic ketoacidosis, lung cancer, kidney failure, peripheral arterial disease with unremitting pain, and interstitial lung disease with cancer. There was no correlation between medication use or diagnosis use and metabolites.

2.2. EBC collection

Breath collection was performed using a custom EBC sampler previously used and described in several studies [7, 11, 28–31]. Volunteers did not eat or drink for 1 h prior to breath collection. Briefly, participants breathed tidally for 15–20 min through a disposable valved mouthpiece (no nose clip) connected to a trap that passively separates saliva and larger contaminants. The trap is attached to a glass tube surrounded by dry ice at −78 °C, achieving temperatures that condensate the exhaled breath and aerosols in the tube. After the subject finished breathing, the EBC was retrieved from the tube and stored in a 10 mL vial at −80 °C until analysis. Mouthpiece and filters were disposed as medical waste after each EBC collection, and all device parts were disinfected with water and ethanol solutions (x3 times) before each use.

2.3 EBC SARS-CoV-2 inactivation and sample preparation

Before preparing the EBC to analyze, samples were treated with 50% acetonitrile to fully inactivate SARS-CoV-2 and make them safe to process following a previous study [6]. For this, 300 μL (or maximum volume collected if < 300 μL) of thawed EBC were aliquoted to a 10 mL glass amber vial. Then, 3 mL of acetonitrile and 2.7 mL of water were added to the sample, together with an isotopically labeled internal standard mixture, the samples were vortexed for 30 s and incubated for 15 min at room temperature. After that time, samples were dried with nitrogen to remove organic solvent, and the aqueous-based EBC was then, mixed and frozen for 30–60 min at −80 °C. Frozen EBC samples were lyophilized until completely dry. Dried extracts were reconstituted with 60 μL of mobile phase (95% water in

acetonitrile) containing an internal standard (30 ng/mL CUDA), vortexed, sonicated for 10 min at 4 °C and centrifuged at 13,000 rpm for 10 min at 4 °C. Supernatant was stored at −80 °C until LC-MS analysis.

Pooled quality controls (QCs) were also prepared with each batch of samples by mixing healthy matrices and spiking it with known concentrations of oxylipins standard mix (targeted compounds). All QCs and blanks (non-spiked samples) were prepared following same sample preparation previously described. Targeted compounds used are reported elsewhere [29] with names, molecular formula, exact masses, LC-MS retention times and are compounds related to inflammation and oxidative stress, which are involved in cyclooxygenase (e.g. prostaglandins and thromboxanes), lipoxygenase (e.g. 5-, 12-, 15-HETE, leukotrienes, DiHETEs, HEPE, etc.), and cytochrome P450 (e.g. HETEs, EETs, DiHOMEs, etc.) pathways.

2.4. Instrumental analysis

LC-MS analyses were performed using an Agilent 1290 series HPLC system with An InfinityLab Poroshell 120 EC-C18 column (3.0 mm × 50 mm, 2.7 μm) (Agilent Technologies, Palo Alto, CA, US) coupled with an Agilent 6530 quadrupole-time of flight (qTOF) mass spectrometer (Agilent Technologies, Santa Clara, CA, USA). 20 uL of samples were injected into de column using an autosampler at 5 °C. Compound separation was achieved using gradient of solvent, with water (A) and acetonitrile (B), both with 0.1% formic acid during a total run time of 30 min.

An electrospray ionization (ESI) source was used with an Agilent Jet Stream nebulizer. Samples were run twice, one in positive and one in negative ESI mode, with a mass ranges of 60–1000 and 100 to 970 m/z for positive and negative, respectively. However, some samples were injected twice in positive mode and not injected in negative. ESI was operated at 250 °C with ionization set at 3000(+)/4000(−) V and fragmentor voltage at 130 V. Nebulizer gas pressure, temperature and drying gas flow rate were set at 45 psi, 400 °C and 10 L/min. All ions MS/MS mode was performed at collision energies of 0 and 15 V. Mass spectra were acquired at a scan rate of 2 spectra/s.

2.5. Chemometric analysis

Preliminary raw data was initially qualitatively checked with Agilent's Mass Hunter Qualitative Analysis B.06.00 software. Data analysis was then performed using univariate and multivariate statistical analysis on the qualitative and quantitative results to determine significant differences among the screened metabolites. Data was obtained with Agilent's Mass Hunter Quantitative (qTOF) Analysis B.07.00 software, and compounds were identified, confirmed, and integrated using accurate mass, retention time and MS/MS information. All detected compounds were quantified using standard calibration curves and responses were corrected with internal standard signals. QCs were used to determine the validity of the calibrations. All missing values were replaced by the LOD/10 and final dataset was log transformed to correct data heteroscedasticity [32].

Resulting dataset was analyzed using Excel, MATLAB R2017a and PLS Toolbox V8.6.2 software. Principal component analysis (PCA) was initially used to overview information,

visualize differences between sample groups and detect potential outliers. PCA projects the data maximum variance based on orthogonal variables, in a linear additive way reducing the dimensionality of the data set. Partial Least-Squares Discriminant Analysis (PLS-DA) was later used as a supervised technique that uses the metabolites information to maximize the discrimination between groups of samples. PLS-DA models maximum covariance between datasets and defined sample class, separating the different groups studied based on their metabolite features [33, 34]. The accuracy of the PLS-DA models was defined by area under the curve (AUC) values of the receiver operating characteristic (ROC) curves, as well as sensitivity and specificity. Models were evaluated using multiple test-validations (n = 100) by randomly dividing the samples into two cohorts composed of 66% training and 33% validation subjects.

To assess the significance of the detected compounds we used comparative Wilcoxon's rank sum test and Volcano plot, providing a quick dissemination based on compound fold changes (FC). Volcano Plots identified features with p-values less than 0.5 and FC values higher than 2. Potential biomarkers for to differentiate case from control groups were selected according to the variable importance in the projection (VIP) values. VIPs summarize the contribution that each feature makes to the model, and values higher than 1 are considered relevant biomarkers.

3. Results and discussion

3.1. Demographics and participants information

In this cross-sectional study, a total of 35 patients were recruited, including 14 acutely hospitalized COVID(+) participants with a positive RT-PCR test and 21 controls, grouped as COVID(−). For COVID(+) patients, we collected the day of last COVID(+) test, however, but we could not determine true onset of the disease. Based on the information we collected, we did not find any correlation using PLS-R between the estimated disease onset and oxylipin levels (Figure S1). Demographic information for the participants enrolled in this study is shown (Table 1). There were 10 males and 4 females in the case group with an average age of 49.7 (range 24–73) years, which is representative of the patients hospitalized with COVID-19 disease in our area [35]. The control group included 13 males and 8 females with an average age of 42.1 (range 19–83) years. Mean EBC volume collected by the participants was 256 (25 – 300) μL and 375 (50 – 300) μL for COVID(+) and COVID(−) subjects, respectively. Medications and doses of medications were documented for all patients, but given the different dosing times and the variable drug half-lives, we were unable to draw any clear conclusions of the effect of drugs on the oxylipins observed in EBC.

3.2. COVID effect on specific oxylipins

We found 24 of a total of 55 oxylipins were identified in the EBC samples and could be quantified with values over the LOD of the method. Although most of the compounds were detected at concentrations below 0.5 ng/mL in the EBC, some of them (8-deoxyguanosine and prostaglandin A2 (PGA2)) were detected at higher concentrations with averages greater than 1 ng/mL throughout the samples, and reaching values of 11 ng/mL in some cases.

All compound concentrations were corrected by IS and volume of EBC used in sample preparation step.

A PCA approach was initially used to assess metabolite differences and intra-group variations between the case and control group (Figure 1a). We observed good separation between groups by PCA, with clear differentiation between COVID (+) and COVID (−) subjects. Also hospitalized patients were differentiated from non-hospitalized ones. The sample separation was clearly enhanced when using a PLS-DA supervised method (Figure 1b), still showing differences by hospitalized groups. For that, we performed 100 model iterations using random split data between calibration and validation sets (66% samples in calibration set). All iterations were averaged, and standard deviation values were determined for AUC, sensitivity, and specificity. We achieved an AUC of 0.92 (±0.08), and sensitivity and specificity were both above 0.8, with 0.88 (±0.15) and 0.81 (±0.14), respectively. For the variables, we looked for breath EBC metabolite compounds with significant differences, considering VIPs higher than 1, p-values lower than 0.05 and FC values lower than −2 or higher than 2. This is reflected in Figure 1c, where a Volcano plot shows compounds with positive FC values (log2(ratio)) were associated with up-regulation by COVID infection, and compounds with negative FC were defined as down-regulated. Up-regulation by COVID means that the average concentrations calculated on the group of COVID(+) were higher to the ones on COVID (−). Figure 1d shows the dysregulations found for all the 24 oxylipins detected. All targeted inflammatory compounds showed higher concentrations in EBC from COVID(+) participants (up-regulated), but only 10 of those showed strong statistically significative differences (*). No targeted inflammatory compounds were downregulated from COVID(+) participants. Specific regulations considering hospitalizations in COVID (−) subjects are presented in Figure S1, where all of the ten highlighted biomarkers of inflammation present downregulation from COVID (+), showing lower concentrations in COVID (−) subjects disregarding their hospitalization status.

Table 2 shows a list of the 24 detected targeted inflammatory compounds with the corresponding chemical name, monoisotopic mass, retention time, molecular formula, and upregulation based on COVID positivity. Ranking of the compounds by significance was determined by VIP scores, p-values and FC values. Prostaglandins A2 and D2, LXA4, 5-HETE, 12-HETE, 15-HETE, 5-HEPE, 9-HODE, 13-oxoODE and 19(20)-EpDPA, were the 10 inflammatory eicosanoid compounds statistically-significantly upregulated based on COVID positivity; however, all measured inflammatory compounds were higher in COVID(+) patients.

Among the individual markers, 15(S)-HETE is considered a major metabolite from arachidonic acid from the 15-lipoxygenase pathway [36], and 13-oxoODE that is putatively linked to the maturation of reticulocytes to erythrocytes through the activity of 15-LOX [37–41]. From these eicosanoid inflammatory biomarkers, some have already been associated with dysregulation due to SARS-CoV2, and a subset of them are known to be formed in macrophages during the response to infection [42]. Oxylipin increases have also been reported in blood using similar metabolomics approaches as our current study [43], and are strongly associated with disease severity in that report. Another report summarizes similar inflammatory responses from the cytokine storm in COVID(+) patients [44].

We found several other reports of blood-based measurements of oxylipins upregulated by SARS-CoV-2 infection: prostaglandin D2 [45]; anti-inflammatory lipoxin LXA4 [46, 47]; 5-HETE [48]; and 12-HETE [48]. Interestingly, we did not find reports of prostaglandin A2 upregulated in blood due to COVID, nor reports of 15-HETE nor 9-HODE nor 13-oxoODE nor 19(20)-EpDPA dysregulation in COVID(+) patients. However, there are reports diminishing levels of 5-HEPE after a single infusion of the therapy Remdesivir™ in rats [49]. Other therapies have also been reported decreased of some of the 10 significant eicosanoids on our Table 2 list [49–52], suggesting and reinforcing those inflammatory pathways represent clinically significant therapy opportunities.

As we reflect on our results, we note that all of our COVID(+) patients were hospitalized, indicating high clinical severity. We would like to note these subjects were not longitudinally sampled, and they were all at different stages of disease progression and/or response to therapies (sometimes drug therapies) when we obtained EBC samples from them. Another limitation of our study was our lack of knowledge about duration of disease and the effects of disease duration on oxylipin levels. Still, based on the information we collected, we did not find any correlation between the estimated days of COVID-19 and oxylipin levels in breath.

As such, we suggest future EBC breath studies for viral respiratory pathogens may benefit from attempting to categorize disease progression as a correlating factor, which may yield even more nuanced statistically-significant target biomarkers of interest. As inflammation in initiated upon infection and followed through to resolution, there is a delicate balance of arachidonic acid metabolism. EBC inflammation biomarker monitoring may have a role to play in personalized medicine approaches to SARS-CoV-2 therapy selection in the future.

4. Conclusions

We measured and quantified 24 inflammatory biomarkers in the exhaled breath condensate of COVID(−) and COVID(+) subjects. Of these, all were higher in those infected, and 10 of these were statistically significant between groups. A total of 4 of these oxylipins were previously reported upregulated in infected patients: prostaglandin D2, LXA4, 5-HETE and 12-HETE. Together, all of this information paints a picture of multiple upregulated metabolomic markers associated with severe inflammation in COVID(+) patients. EBC breath analysis that targets these inflammation pathways may yield new insight into therapy and drug pathways, and may provide a new avenue for tracking patient progression and personalized medicine approaches to therapies.

Supplementary Material

Refer to Web version on PubMed Central for supplementary material.

Acknowledgements

This work was partially supported by: NIH awards 1U18TR003795, 4U18TR003795, 1U01TR004083 and UL1 TR001860; UG3-OD023365; 1P30ES023513-01A1 [NJK, CED]; the Department of Veterans Affairs award I01 BX004965-01A1 [NJK, CED]; the University of California Tobacco-Related Disease Research Program award T31IR1614 [NJK, CED]; the National Science Foundation award 2200221 [CED], and the Department of Energy.

The contents of this manuscript are solely the responsibility of the authors and do not necessarily represent the official views of the funding agencies. Research was sponsored by the Office of the Secretary of Defense and was accomplished under Agreement Number W911NF-17-3-0003 [CED]. The views and conclusions contained in this document are those of the authors and should not be interpreted as representing the official policies, either expressed or implied, of the Office of the Secretary of Defense of the U.S. Government. The U.S. Government is authorized to reproduce and distribute reprints for Government purposes notwithstanding any copyright notation herein. The authors declare no competing financial interest.

References

1. WHO, WHO Coronavirus disease (COVID-19) situation reports. 2022.
2. Borczuk AC, et al. , COVID-19 pulmonary pathology: a multi-institutional autopsy cohort from Italy and New York City. Modern Pathology, 2020. 33(11): p. 2156–2168. [PubMed: 32879413]
3. CDC. Interim Guidelines for Collecting and Handling of Clinical Specimens for COVID-19 Testing. 2022 [cited 2022 November]; Available from: https://www.cdc.gov/coronavirus/2019-nCoV/lab/guidelines-clinical-specimens.html.
4. Bhimraj A, et al. , Infectious Diseases Society of America Guidelines on the Treatment and Management of Patients With Coronavirus Disease 2019 (COVID-19). Clinical Infectious Diseases, 2020.
5. Wölfel R, et al. , Virological assessment of hospitalized patients with COVID-2019. Nature, 2020. 581(7809): p. 465–469. [PubMed: 32235945]
6. Hu S, et al. , Inactivation of SARS-CoV-2 in clinical exhaled breath condensate samples for metabolomic analysis. Journal of Breath Research, 2022. 16(1): p. 017102.
7. Borras E, et al. , Detecting opioid metabolites in exhaled breath condensate (EBC). Journal of Breath Research, 2019. 13(4): p. 046014. [PubMed: 31349234]
8. Pasamontes A, et al. , Noninvasive Respiratory Metabolite Analysis Associated with Clinical Disease in Cetaceans: A Deepwater Horizon Oil Spill Study. Environmental Science & Technology, 2017. 51(10): p. 5737–5746. [PubMed: 28406294]
9. Borras E, et al. , Exhaled breath condensate methods adapted from human studies using longitudinal metabolomics for predicting early health alterations in dolphins. Anal Bioanal Chem, 2017. 409(28): p. 6523–6536. [PubMed: 29063162]
10. Gould O, et al. , Breath analysis for detection of viral infection, the current position of the field. J Breath Res, 2020. 14(4): p. 041001. [PubMed: 32531777]
11. Konstantin OZ, et al. , Human breath metabolomics using an optimized non-invasive exhaled breath condensate sampler. Journal of Breath Research, 2017. 11(1): p. 016001.
12. Davis MD and Montpetit AJ, Exhaled Breath Condensate: An Update. Immunology and Allergy Clinics of North America, 2018. 38(4): p. 667–678. [PubMed: 30342587]
13. Hunt J, Exhaled breath condensate: an overview. Immunol Allergy Clin North Am, 2007. 27(4): p. 587–96; v. [PubMed: 17996577]
14. Sawano M, et al. , RT-PCR diagnosis of COVID-19 from exhaled breath condensate: a clinical study. Journal of Breath Research, 2021. 15(3): p. 037103.
15. Li X, et al., Detecting SARS-CoV-2 in the Breath of COVID-19 Patients. 2021. 8.
16. Ma J, et al., Exhaled breath is a significant source of SARS-CoV-2 emission. NOT PREER-REVIEWED, 2020.
17. Duan C, et al. , Efficient Detection of Severe Acute Respiratory Syndrome Coronavirus 2 (SARSCoV-2) from Exhaled Breath. J Mol Diagn, 2021. 23(12): p. 1661–1670. [PubMed: 34600137]
18. Sawano M, et al. , SARS-CoV-2 RNA load and detection rate in exhaled breath condensate collected from COVID-19 patients infected with Delta variant. Journal of Breath Research, 2022. 16(3): p. 036006.
19. Ryan DJ, et al. , Use of exhaled breath condensate (EBC) in the diagnosis of SARS-COV-2 (COVID-19). Thorax, 2021. 76(1): p. 86–88. [PubMed: 33097604]
20. Zhou L, et al. , Breath-, air- and surface-borne SARS-CoV-2 in hospitals. Journal of Aerosol Science, 2021. 152: p. 105693. [PubMed: 33078030]

21. Wu D, et al. , Plasma metabolomic and lipidomic alterations associated with COVID-19. National Science Review, 2020. 7(7): p. 1157–1168. [PubMed: 34676128]
22. Barberis E, et al. , Metabolomics Diagnosis of COVID-19 from Exhaled Breath Condensate. Metabolites, 2021. 11(12).
23. Montuschi P and Barnes PJ, Analysis of exhaled breath condensate for monitoring airway inflammation. Trends in Pharmacological Sciences, 2002. 23(5): p. 232–237. [PubMed: 12008001]
24. Shen B, et al. , Proteomic and Metabolomic Characterization of COVID-19 Patient Sera. Cell, 2020. 182(1): p. 59–72.e15. [PubMed: 32492406]
25. Song J-W, et al. , Omics-Driven Systems Interrogation of Metabolic Dysregulation in COVID-19 Pathogenesis. Cell Metabolism, 2020. 32(2): p. 188–202.e5. [PubMed: 32610096]
26. Li X, et al. , Metabolic profile of exhaled breath condensate from the pneumonia patients. Experimental Lung Research, 2022. 48(4–6): p. 149–157. [PubMed: 35708062]
27. McCartney MM, et al. , Predominant SARS-CoV-2 variant impacts accuracy when screening for infection using exhaled breath vapor. Communications Medicine, 2022. 2(1): p. 158. [PubMed: 36482179]
28. Borras E, et al. , Exhaled breath biomarkers of influenza infection and influenza vaccination. J Breath Res, 2021. 15(4).
29. Alexander James S, et al. , Portable exhaled breath condensate metabolomics for daily monitoring of adolescent asthma. Journal of Breath Research, 2019.
30. Aksenov AA, et al. , Analytical methodologies for broad metabolite coverage of exhaled breath condensate. Journal of Chromatography B, 2017.
31. Zamuruyev KO, et al. , Power-efficient self-cleaning hydrophilic condenser surface for portable exhaled breath condensate (EBC) metabolomic sampling. Journal of Breath Research, 2018. 12(3): p. 036020. [PubMed: 29771240]
32. Gorrochategui E, et al. , Data analysis strategies for targeted and untargeted LC-MS metabolomic studies: Overview and workflow. TrAC Trends in Analytical Chemistry, 2016. 82: p. 425–442.
33. Sumner LW, Urbanczyk-Wochniak E, and Broeckling CD, Metabolomics data analysis, visualization, and integration. Methods Mol Biol, 2007. 406: p. 409–36. [PubMed: 18287705]
34. Want E and Masson P, Processing and analysis of GC/LC-MS-based metabolomics data. Methods Mol Biol, 2011. 708: p. 277–98. [PubMed: 21207297]
35. CDPH. COVID-19 Age, Race and Ethnicity Data. 2022 [cited 2022 November]; Available from: https://www.cdph.ca.gov/Programs/CID/DCDC/Pages/COVID-19/Age-Race-Ethnicity.aspx.
36. Nadel JA, et al. , Immunocytochemical localization of arachidonate 15-lipoxygenase in erythrocytes, leukocytes, and airway cells. J Clin Invest, 1991. 87(4): p. 1139–45. [PubMed: 2010530]
37. Earles SM, et al. , Metabolism of oxidized linoleic acid: characterization of 13-hydroxyoctadecadienoic acid dehydrogenase activity from rat colonic tissue. Biochim Biophys Acta, 1991. 1081(2): p. 174–80. [PubMed: 1998735]
38. Hayakawa M, et al. , Proposal of leukotoxin, 9,10-epoxy-12-octadecenoate, as a burn toxin. Biochemistry international, 1990. 21(3): p. 573–579. [PubMed: 2222499]
39. Ma S, et al. , Does aspirin have an effect on risk of death in patients with COVID-19? A meta-analysis. Eur J Clin Pharmacol, 2022. 78(9): p. 1403–1420. [PubMed: 35732963]
40. Hammock BD, et al. , Eicosanoids: The Overlooked Storm in Coronavirus Disease 2019 (COVID-19)? Am J Pathol, 2020. 190(9): p. 1782–1788. [PubMed: 32650004]
41. Manickam M, Meenakshisundaram S, and Pillaiyar T, Activating endogenous resolution pathways by soluble epoxide hydrolase inhibitors for the management of COVID-19. Arch Pharm (Weinheim), 2022. 355(3): p. e2100367. [PubMed: 34802171]
42. Radmark O, Formation of eicosanoids and other oxylipins in human macrophages. Biochem Pharmacol, 2022. 204: p. 115210. [PubMed: 35973581]
43. Karu N, et al. , Plasma Oxylipins and Their Precursors Are Strongly Associated with COVID-19 Severity and with Immune Response Markers. Metabolites, 2022. 12(7).
44. Biagini D, et al. , MS-based targeted profiling of oxylipins in COVID-19: A new insight into inflammation regulation. Free Radic Biol Med, 2022. 180: p. 236–243. [PubMed: 35085774]

45. Conti P, et al. , Mast cells activated by SARS-CoV-2 release histamine which increases IL-1 levels causing cytokine storm and inflammatory reaction in COVID-19. J Biol Regul Homeost Agents, 2020. 34(5): p. 1629–1632. [PubMed: 32945158]

46. Jamali F, et al. , LipoxinA4 as a Potential Prognostic Marker of COVID-19. J Lipids, 2022. 2022: p. 8527305. [PubMed: 35812307]

47. Das UN, Bioactive Lipids in COVID-19-Further Evidence. Arch Med Res, 2021. 52(1): p. 107–120. [PubMed: 32981754]

48. He X, et al. , COVID-19 induces new-onset insulin resistance and lipid metabolic dysregulation via regulation of secreted metabolic factors. Signal Transduct Target Ther, 2021. 6(1): p. 427. [PubMed: 34916489]

49. Du P, et al. , Eicosanoid Metabolomic Profile of Remdesivir Treatment in Rat Plasma by High-Performance Liquid Chromatography Mass Spectrometry. Front Pharmacol, 2021. 12: p. 747450. [PubMed: 34658883]

50. Roy Wong LY, et al. , Eicosanoid signaling as a therapeutic target in middle-aged mice with severe COVID-19. bioRxiv, 2021.

51. Sokolowska M, et al. , Effects of non-steroidal anti-inflammatory drugs and other eicosanoid pathway modifiers on antiviral and allergic responses: EAACI task force on eicosanoids consensus report in times of COVID-19. Allergy, 2022. 77(8): p. 2337–2354. [PubMed: 35174512]

52. Chiang KC, et al. , Ramatroban for chemoprophylaxis and treatment of COVID-19: David takes on Goliath. Expert Opin Ther Targets, 2022. 26(1): p. 13–28. [PubMed: 35068281]

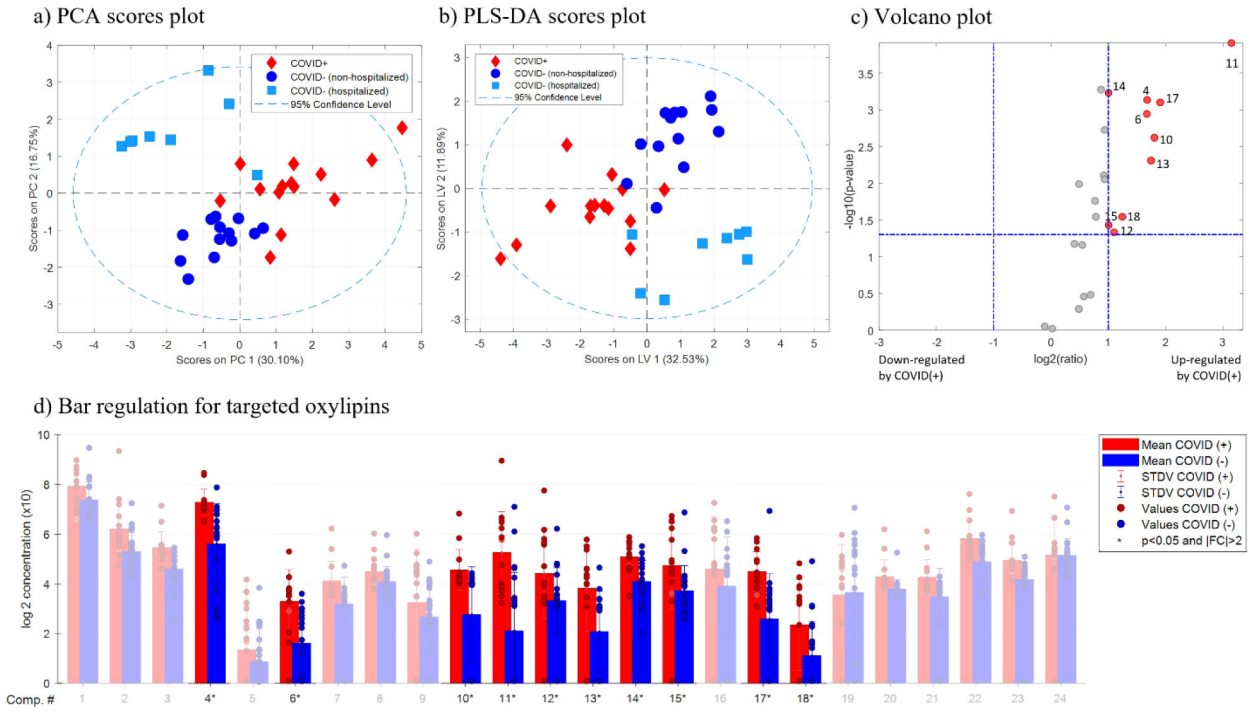

Figure 1.

Results from targeted oxylipin quantification, where: (a) is a PCA scores plot showing differences between COVID(+) and COVID(−) samples, (b) is a PLS-DA cores plot with defined differences between participants, and (c) is a volcano plot targeted metabolites, showing log2 mean ratio fold-change (x-axis) of relative abundance of each compound between COVID (+) and COVID (−) versus p-value of each compound (y-axis). Compounds with fold-change >2 and $p<0.05$ are labeled and highlighted in red. (d) is a bar plot showing differences between samples group averages, expressed as log2 concentrations. Asterisks (*) correspond to compounds with significative differences between COVID(+) and COVID(−) ($p<0.05$).

Table 1.

Demographic and participants information. Percentages are reported with total numbers in parentheses

	COVID(+)	COVID(−)
Number of subjects	40% (14)	60% (21)
Age (mean ± standard deviation)	49.7 ± 16.7	42.1 ± 23.3
Biological sex, male	71.4% (10)	61.9% (13)
Race		
American Indian or Alaska Native	7.1% (1)	0.0% (0)
Asian or Pacific Islander	0.0% (0)	23.8% (5)
Black or African American	14.3% (2)	9.5% (2)
Caucasian	28.6% (4)	47.6% (10)
Other	42.9% (6)	9.5% (2)
Native Hawaiian	7.1% (1)	0.0% (0)
Unknown/Declined to State	0.0% (0)	9.5% (2)
Hispanic, Latino or Spanish origin	42.9% (6)	0.0% (0)
EBC volume (uL)	256 (25 – 300)	375 (50 – 300)

Table 2.

List of targeted oxylipins quantified in EBC samples. Described number of compound (#), name, monoisotopic mass, retention time, formula and COVID regulation. Up-regulations with * correspond to compounds presenting significative differences between COVID(+) and COVID(−), defined by VIP > 1, p-values > 0.05, and Fold Change (FC) > 2.

#	Compound ID	Mass	RT	Formula	C0VID regulation	VIP	p-values	FC
1	8-deoxyguanosine	283.0917	0.53	C10H13N505	up	0.5	0.083	1.5
2	6-keto Prostaglandin F1α	370.2355	5.62	C20H3406	up	0.9	0.008	1.9
3	15do-Prostaglandin J2	316.2038	14.50	C20H2803	up	0.9	0.000	1.8
4*	**Prostaglandin A2**	**334.2144**	**9.54**	**C20H30O4**	**up***	**1.3**	**0.000**	**3.2**
5	Prostaglandin B2	334.2144	8.76	C20H3004	up	0.7	0.106	1.4
6*	**Prostaglandin D2**	**352.2250**	**7.40**	**C20H32O5**	**up***	**1.3**	**0.001**	**3.2**
7	Prostaglandin E2 + H2	352.2250	7.37	C20H3205	up	0.9	0.000	1.9
8	Prostaglandin I2	351.2171	5.40	C20H3105-	up	0.5	0.030	1.3
9	11-Dehydro-thromboxane B2	368.2199	7.49	C20H3206	up	0.6	0.075	1.5
10*	**LXA4**	**352.2250**	**8.27**	**C20H32O5**	**up***	**1.4**	**0.000**	**3.5**
11*	**5-HETE**	**320.2351**	**17.54**	**C20H32O3**	**up***	**1.9**	**0.000**	**8.9**
12*	**12-HETE**	**320.2351**	**17.07**	**C20H32O3**	**up***	**1.0**	**0.019**	**2.1**
13*	**15-HETE**	**320.2351**	**16.38**	**C20H32O3**	**up***	**1.3**	**0.001**	**3.3**
14*	**5-HEPE**	**318.2195**	**15.84**	**C20H30O3**	**up***	**1.0**	**0.001**	**2.0**
15*	**9-HODE**	**296.2351**	**16.00**	**C18H32O3**	**up***	**1.0**	**0.006**	**2.0**
16	13-HODE	296.2351	15.85	C18H3203	up	0.5	0.125	1.6
17*	**13-oxoODE**	**294.2195**	**16.56**	**C18H30O3**	**up***	**1.4**	**0.000**	**3.7**
18*	**19(20)-EpDPA**	**344.2351**	**18.09**	**C22H32O3**	**up***	**1.0**	**0.033**	**2.4**
19	14(15)-EpETE	318.2195	17.03	C20H3003	up	0.4	0.588	1.1
20	8(9)-DiHETE	338.2457	14.24	C20H3404	up	0.6	0.000	1.4
21	11(12)-DiHETE	338.2457	13.73	C20H3404	up	0.8	0.011	1.7
22	14(15)-DiHETE	336.2301	11.71	C20H3204	up	0.9	0.004	1.9
23	9,10-DiH0ME	314.2457	12.47	C18H3404	up	0.9	0.002	1.7
24	12,13-DiHOME	314.2457	12.00	C18H3404	up	0.4	0.117	1.0